Materials Science-Poland, Vol. 25, No. 4, 2007

Iron oxide(III) nanoparticles fabricated by electron beam irradiation method

B. ZHAO[1], Y. WANG[1], H. GUO[1], J. WANG[2], Y. HE[2], Z. JIAO[1*], M. WU[2]

[1]Institute of Nanochemistry and Nanobiology, Shanghai University, Shanghai 201800, China

[2]School of Environmental and Chemical Engineering, Shanghai University, Shanghai 201800, P.R. China

Iron oxide(III) nanoparticles were fabricated by the electron beam irradiation method. The structure and morphology of the iron oxide nanoparticles were analyzed by XRD, TEM, AFM and FTIR. Phase transformation temperatures were determined by DSC–TGA. Results showed that the phase transition point and melting point decreased greatly. The size effects were discussed to explain the reason.

Key words: iron oxide(III); electron beam; irradiation; nanoparticles

1. Introduction

Iron oxide(III) is an extensively investigated material because of its magnetic, optical and catalytic properties. It has been used as electrodes in non-aqueous and alkaline batteries [1], as cathodes in brine electrolysis [2], shows photocatalytic properties for N_2 fixation [3], etc. It is possible to change its semiconducting character from n- to p-type by applying an appropriate dopant. Also iron oxide is used to fabricate pigments, sorbents and gas sensors [4].

Iron oxide(III) has been prepared by various methods such as chemical vapour deposition [5], sol-gel processes [6], pulsed laser evaporation [7], reactive sputtering [8], hydrothermal technique [9] and spray pyrolysis [10, 11]. In this paper, electron beam irradiation, a novel method to fabricate nanocrystalline iron oxide(III) has been described. The microstructure, morphology and thermodynamic properties of iron oxide were studied.

*Corresponding author, e-mail: zjiao@shu.edu.cn

2. Experimental

$FeCl_3 \cdot 6H_2O$, NaOH, isopropyl alcohol and polyvinyl alcohol, all of analytical grade, were used to fabricate iron oxide(III) nanoparticles. $FeCl_3 \cdot 6H_2O$ was dissolved in deionized water and the the following solutions were added: 1 M NaOH to adjust pH between 4 and 8, poly(vinyl) alcohol (PVA) to control the nanoparticle sizes and to prevent aggregation as well as isopropyl alcohol (IPA) as scavenger of oxidative radicals ($OH^{\cdot}$).

A GJ-2-II electronic accelerator was used to generate electron beams, working at 2 MeV 10 mA. The solutions were irradiated under electron beam at various doses. After irradiation, the suspensions were left for several hours to allow precipitation. The sediments were collected by centrifuging, and washed several times with deionized water to remove by-products. After vacuum drying at 60 ºC for 12 h, the powders were heat treated at 600 ºC for half an hour to obtain iron oxide nanoparticles.

The particle structure was characterized by a D-MAX-rC X-ray diffraction. The crystallite sizes were calculated based on the X-ray diffraction spectrum using the Scherrer equation. The morphology and microstructure of particles were examined by Hitachi H-800 TEM. In order to study the fine structure of the films, the surface morphology of the film was also examined by a Nanofirst-3000 AFM. Characteristic absorption bands of the powder were investigated by Avatar-370 FTIR. Thermal stability of samples was analyzed by TA SDT Q600 DSC-under dry nitrogen (containing less than 1% of oxygen) at a heating rate of 10 ºC/min from 20 ºC to 1400 ºC.

3. Results and discussion

The XRD pattern of fabricated iron oxide nanoparticles is shown in Fig. 1. The XRD peaks are at $2\theta = 24.16^{o}$, 33.20^{o}, 35.66^{o}, 40.90^{o}, 49.52^{o}, 54.12^{o}, 57.64^{o}, 69.62^{o} and 72.00^{o}. According to JCPDS card (76-1821), the powder is hexagonal α-Fe_2O_3. Calculated from the Scherrer equation, the sizes of crystals ranged from 34.2 nm to 53.9 nm (mean value – 42.5 nm).

The TEM images are shown in Fig. 2. The iron oxide(III) particles have spherical shape morphology, fine dispersion and mean particle sizes between 20 and 60 nm. The nanoparticle sizes observed by TEM are in agreement with those calculated by XRD.

AFM was also used to investigate the morphology and roughness of a nanometer-order of magnitude in an area up to 1 μm^2. Figure 3a shows a representative AFM image of α-Fe_2O_3 nanoparticles by electron beam irradiation. It can be seen that the powders have spherical particles, and the mean size of particles is about 39 nm. Figure 3b is a three-dimensional AFM image of the same sample, all island-like grains are strongly elongated in one direction. The size distribution of nanoparticles is shown in Fig. 3c, α-Fe_2O_3 nanoparticles obtained by electron beam irradiation have mean particle sizes of 39 nm.

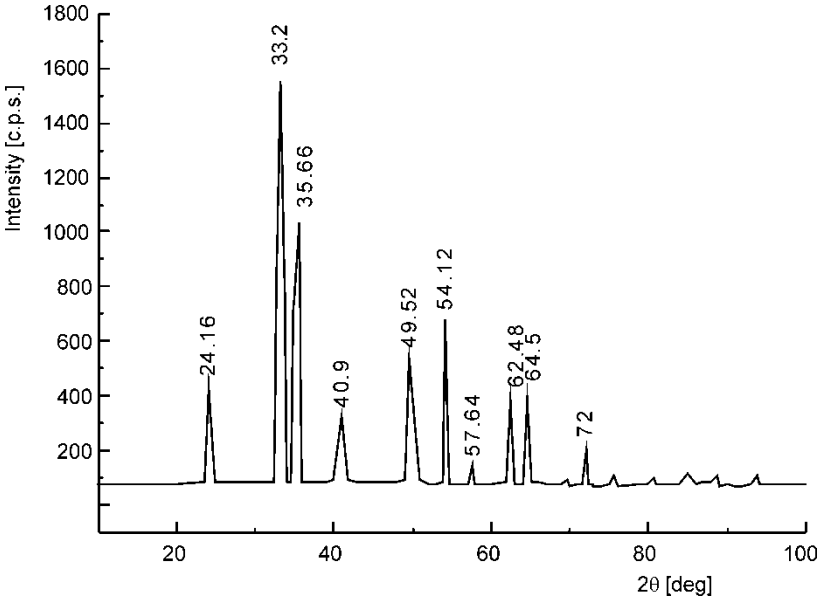

Fig. 1. The XRD pattern of α-Fe_2O_3 powder prepared by electron beam irradiation

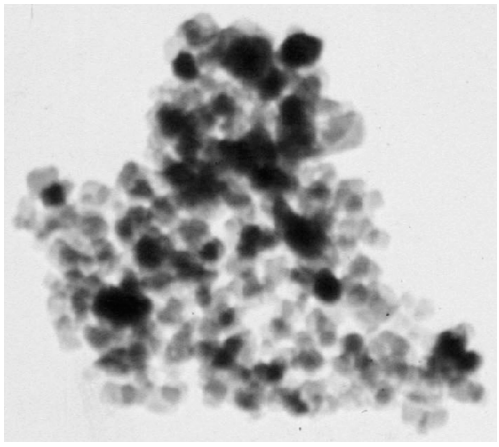

Fig. 2. The TEM morphology of α-Fe_2O_3 powder

The FTIR spectrum of α-Fe_2O_3 powder is shown in Fig. 4. Characteristic absorption bands at 536.57 cm^{-1} and 460.09 cm^{-1} for powder are assigned to α-Fe_2O_3. From the IR data, there is no evidence that α-Fe_2O_3 nanoparticles are contaminated by foreign materials in the system.

DSC/TGA results were shown in Fig. 5. From the TGA curve, the sample dried at 60 ºC undergoes a total weight loss of 25% with four decomposition steps from 20 ºC to 1400 ºC. The weight loss below 200 ºC is due to the removal of loosely bound water of the sample. The decomposition step between 220 and 400 ºC is due to the decomposition of nitrate ions and dehydroxylation of the sample. The third step between

400 and 900 ºC is attributed to the phase transformation from γ-Fe_2O_3 to α-Fe_2O_3. The weight loss over 900 ºC is extremely small.

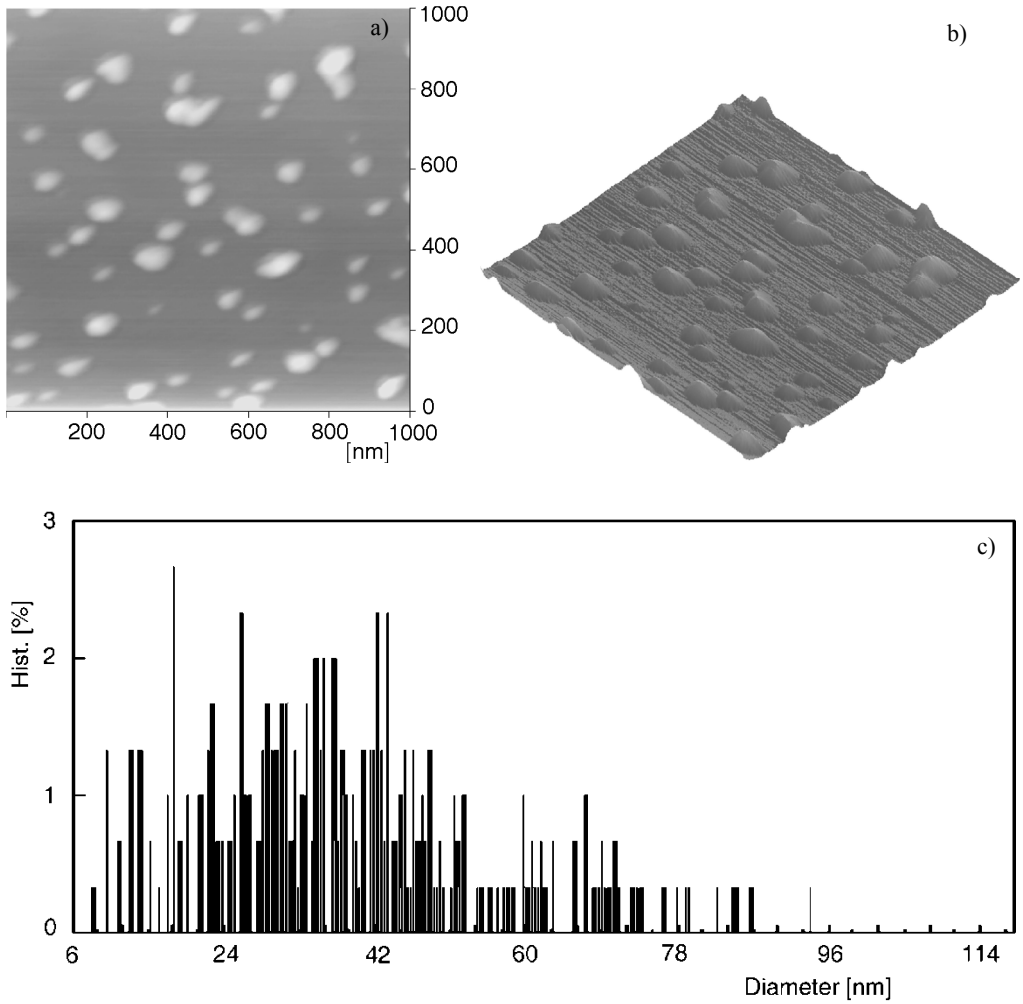

Fig. 3. AFM images of α-Fe_2O_3 powder prepared by electron beam irradiation: a) topography, b) 3D image, c) size distribution

From the DSC curve, two main peaks can be observed at 770 ºC and 1355 ºC during heating up to 1400 ºC indicating that two phase transformations occur. The peak temperature was employed to identify different phase transformation. The exothermic peak at 770 ºC should be ascribed to the phase transformation process of crystal type from γ-Fe_2O_3 (low temperature type) to α-Fe_2O_3 (high temperature type). In previous paper, Trautmann determined the enthalpy difference between γ-Fe_2O_3 and α-Fe_2O_3 as 19.5 kJ /mol [12], In our works, the enthalpy change for the peak at 770 ºC (corresponding to phase transition) is 99.90 J/g, equal to 15.98 kJ/mol. This is because the

nanoparticles have small particle sizes and high surface area, which bring high activity and decrease phase transition energy. The exothermic peak at 1355 ºC is attributed to the phase transformation process of α-Fe_2O_3 from solid to liquid state, lower than the normal melting point of Fe_2O_3, 1530 ºC.

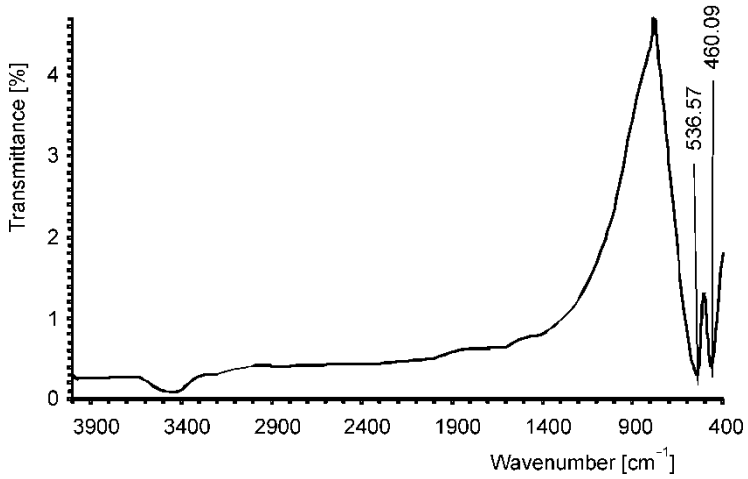

Fig. 4. FTIR spectrum of α-Fe_2O_3 powder

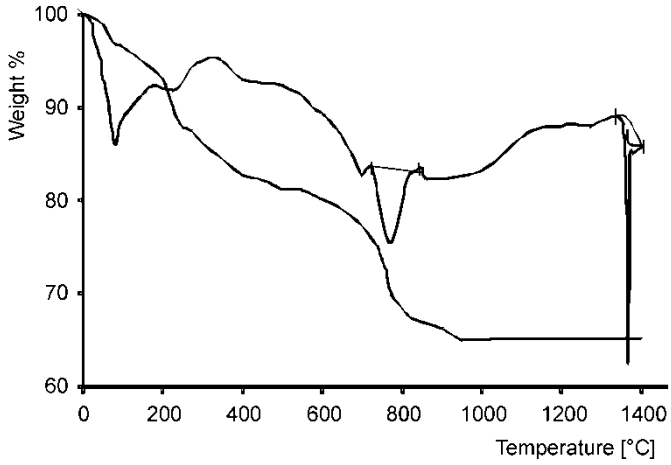

Fig. 5. DSC-TGA curves for α- Fe_2O_3 powder

According to Kelvin equation, $RT\ln(p_r/p) = 2\gamma V_m/r$, the saturated vapour pressure of small particles is higher than that over a flat surface. For nanoparticles, the saturated vapour pressure will be several times higher than that in normal state, which we think will cause the decrease of the melting point.

4. Conclusion

In this paper nanocrystalline iron oxide(III) has been prepared by electron beam irradiation. The optimal experiment condition was obtained at pH 6.0 and 300 kGy irradiation dose. XRD, TEM, AFM and FTIR results shown that the obtained particles by electron beam irradiation method are hexagonal α-Fe_2O_3, nanoparticles have average diameters around 30–60 nm, and have spherical shape morphology, well-degree of dispersion. The phase transition energy and melting point decreased from normal value, which are due to small size effects.

Acknowledgements

The authors gratefully acknowledge support from Shanghai Committee of Science & Technology Qimingxin project (05QMX1423, 06QH14005), Shanghai Committee of Education (07ZZ11, 50578090) and Shanghai Leading Academic Disciplines (T0105).

References

[1] KENICHI S., AKINIDE J., KIYOHIDE T., Japan Patents, 61 (1986), 147.
[2] KEIJI K., ITSUAKI M., Japan Patents, 79 (1979), 78.
[3] KHADAR M.M., LICHTIN N.N., VURNES G.H., SALMENON M., SOMORAJ G.A., Langmuir, 3 (1987), 303.
[4] KULKARNI S.S., LOKHANDE C.D., Mater. Chem. Phys., 82 (2003), 151.
[5] CHAI C.C., PENG J., YAN B.P., Sensors Actuators B, 34 (1996), 412.
[6] ZHU Y., QIAN Y., Mater. Res. Bull., 29(1994), 377.
[7] JOSHI S., NAWATHEY R., KOINKAR V.N., J. Appl. Phys., 64 (1988), 5647.
[8] WILHELM S.M., YUN K.S., BALLANGER L.W., HACKERMAN N., J. Electrochem. Soc., 126 (1979), 419.
[9] CHEN Q.W., QIAN Y.T., Mater. Res. Bull., 30 (1995), 443.
[10] QIAN Y.T., NIU C-M., HANNIGAN C., Yang S., J. Solid State Chem., 92 (1991), 208.
[11] XIE Y., WANG W., QIAN Y.T., J. Cryst. Growth, 167 (1996), 656.
[12] MAJZLAN J., NAVROTSKY A., SCHWERTMANN U., Geochim. Cosmochim. Acta. 68(2004),s1049.

Received 23 July 2007